



## Do in situ forming PLG/NMP implants behave similar *in vitro* and *in vivo*? A non-invasive and quantitative EPR investigation on the mechanisms of the implant formation process

Sabine Kempe, Hendrik Metz, Karsten Mäder\*

Institute of Pharmacy, Pharmaceutics and Biopharmaceutics Division, Martin Luther University Halle-Wittenberg, Halle 06120, Germany

### ARTICLE INFO

#### Article history:

Received 7 April 2008

Accepted 12 June 2008

Available online 17 June 2008

#### Keywords:

Poly(lactide-co-glycolide)

EPR

ESR

In situ forming implants

In vitro–in vivo correlation

### ABSTRACT

Electron paramagnetic resonance (EPR) spectroscopy was applied to monitor non-invasively the formation of in situ forming implants *in vitro* and *in vivo* after the administration of poly(lactide-co-glycolide) (PLGA)/N-methyl-pyrrolidone (NMP) solutions. The nitroxide spin probe 4-benzoyloxy-2,2,6,6-tetramethylpiperidine-1-oxyl (TB) was incorporated in polymer solutions and samples were incubated in 0.1 M phosphate buffer (pH 7.4) at 37 °C or injected subcutaneously in the femoral of BALB/c mice. EPR permitted the direct and continuous determination of the NMP-water exchange during implant formation both *in vitro* and in living mice. The formation of the implant structure followed a two phase mechanism: over 75% of the polymer precipitated immediately after injection within the first 30 min and formed a solid shell. The subsequent moderate solidification of the implants was governed by diffusion and was completed after 24 h. The replacement of the organic solvent NMP by water was determined by polarity shifts within the implant and could be quantified. Both the kinetic of NMP-water exchange and polymer precipitation showed good *in vitro*–*in vivo* correlation.

© 2008 Elsevier B.V. All rights reserved.

### 1. Introduction

Parenteral depot systems have received significant research interest in the recent years, due to the steadily increasing number of biotechnology-based drugs and compounds which cannot be administered via the oral route. Various types of parenteral dosage forms are available, such as emulsions [1], liposomes [2], micelles [3], implants [4] and microparticles [5]. Their general advantages are localized or systemic prolonged drug delivery periods, drug dosage reduction along with decrease of undesirable side effects and diminished frequency of application. A major development of the past decade has been the fabrication of implantable delivery systems based on biocompatible or biodegradable polymers. These implants were injected subcutaneously by minor surgery and in case of non-biodegradable polymers, the implants had to be removed after the release periods. To overcome these limitations an increasing number of injectable and biodegradable in situ forming systems have been developed as alternatives [6–8]. These systems are generally liquid or semisolid polymeric formulations that form in situ semi-solid or solid depots after injection. Biodegradable implants formed from injectable fluids have several advantages compared to pre-shaped parenteral depot systems. The application of in situ forming implants (ISFI) is less

invasive and painful compared to common implants leading to an improved patient compliance and comfort. The manufacturing conditions are mild and un-complicated, especially for sensitive drug molecules like proteins. ISFI can be classified according to their mechanisms of implant formation: thermoplastic pastes [9], in situ cross-linked polymer systems [10], thermally induced gelling systems [11] and in situ polymer precipitation systems [12,13]. Only in situ polymer precipitation systems have become commercial available so far as 1 to 6 months depot formulations of leuprolide for the treatment of prostate cancer (ELIGARD®) [14]. This approach employs the biodegradable polymer poly(lactide-co-glycolide) (PLGA) dissolved in the water miscible, physiological compatible organic solvent N-methyl-2-pyrrolidone (NMP) [15]. Prior to injection the drug is added and forms a solution or suspension. After subcutaneous injection of the formulation into the body the organic solvent dissipates into the surrounding tissue as water penetrates in. This leads to phase separation and precipitation of the polymer forming a depot at the injection site. The way the implant solutions respond to its physiological surroundings determines their release characteristics and morphology. A critical point in the design and optimization of such drug delivery systems is to understand this interplay between the biological system, the drug and the delivery device. Due to the difficulty to study such complex systems, the knowledge for the *in vivo* conditions is still very limited. The influence of several formulation parameters, like poly(lactide-co-glycolide) type, type of solvent or co-solvent and additives, have been studied in detail *in vitro*

\* Corresponding author. Tel.: +49 345 55 25167; fax: +49 345 55 27029.  
E-mail address: [karsten.maeder@pharmazie.uni-halle.de](mailto:karsten.maeder@pharmazie.uni-halle.de) (K. Mäder).

[16,17]. McHugh and co-workers developed a dark ground video imaging technique that enables to visualise diffusion, liquid–liquid phase separations and gel formation processes and quantified the phase inversion dynamics of several PLGA solutions [18,19]. However this technique is limited to thin films, a small time scale (minutes to few hours) and *in vitro* experiments. Most frequently applied methods for the *in vivo* characterization of implants, such as chromatography and microscopy require the surgical extraction and special sample preparation that may lead to artefacts. In addition, these procedures exclude continuous studies with the same sample on a single animal. Therefore the *in vivo* knowledge concerning the formation of *in situ* forming implants is still very limited. It was the aim of the present study to develop a non-invasive method to monitor phase inversion dynamics and implant formation online *in vitro* and *in vivo*. For this purpose, electron paramagnetic resonance spectroscopy (EPR, also known as electron spin resonance, ESR) was selected as a suitable method. The EPR method allows the non-invasive detection of the interaction of paramagnetic compounds, consisting of one or more unpaired electrons, with their direct environment also in complex and non-transparent samples. Using nitroxides as spin probes or spin labels unique information about the microviscosity, micropolarity and spatial distribution inside drug delivery systems can be obtained. A recent review summarises the principles and applications of EPR spectroscopy and imaging in drug delivery [20]. Thus water penetration, drug release and polymer erosion of polymeric implants have been monitored *in vitro* and *in vivo* [21,22]. Furthermore special designed nitroxides permit the measurement of proton activity [23]. This method has been used to detect the microacidity and to follow pH-gradients inside degrading polymers [24] and tablets [25]. In this study we investigated a system based on the solvent removal precipitation of the water insoluble PLGA due to the fact that co-polyesters of lactic and glycolic acid are the most relevant polymers with respect to their clinical use [26]. NMP was chosen as the organic phase as there are several products on the market [14]. The lipophilic stable nitroxyl radical 4-benzoyloxy-2,2,6,6-tetramethylpiperidine-1-oxyl (Tempolbenzoate, TB) was used as a model drug. TB is poorly water soluble ( $\log P=2.46$ ), comparable to Griseofulvin ( $\log P=2.18$ ) and Diazepam ( $\log P=2.92$ ) [27].

## 2. Materials and methods

### 2.1. Sample preparation

Poly(D,L-lactide-co-glycolide) (PLGA, 50:50 molar ratio D,L-lactide: glycolide, Mw 34,000; Resomer RG503H, Boehringer Ingelheim, Germany) was dissolved in N-methyl-2-pyrrolidone (NMP, Merck, Germany) upon stirring at room temperature, which lead to a clear solution and a final concentration of 30% (w/v). The lipophilic stable nitroxyl radical 4-benzoyloxy-2,2,6,6-tetramethylpiperidine-1-oxyl (Tempolbenzoate, TB, Sigma, Germany) was incorporated in the PLGA-NMP-solution up to a final concentration of 5 mmol per kg PLGA. For calibration measurements TB was dissolved in mixtures of NMP and phosphate buffer (pH 7.4) at a concentration of 0.25 mM. Aliquots of 1 ml were taken and measured at 1.1–1.3 GHz EPR spectrometer (MagnetTech, Germany) in case for *in vivo* and *in vitro* conditions. The values of the hyperfine splitting  $2a_N$  (distance 1st to 3rd peak) were determined from the spectra and were plotted against the concentration of NMP in different NMP-buffer mixtures. The obtained calibration curve (Fig. 1) show that the hyperfine splitting parameter  $2a_N$  corresponds with the NMP concentration in the dilution series. The regression coefficient for the calibration curve is  $>0.99$ . The presented EPR method is therefore suitable to determine dissolution induced changes in micropolarity.

All measurements were performed in triplicate; data are reported as mean  $\pm$  SEM. The “Cu3 v.6.1” program (MagnetTech, Germany) was used for data recording. The programs “Analysis” (MagnetTech, Germany) and “Nitroxide Spectra Simulation – Freeware Version

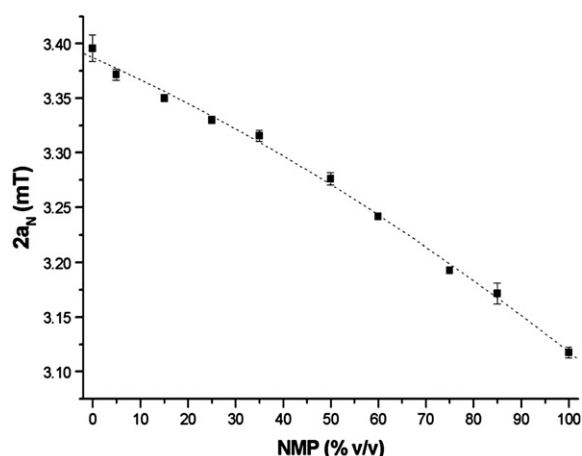


Fig. 1. Dependence of the hyperfine splitting  $2a_N$  in different NMP-buffer mixtures.

4.99–2005” (“Jozef Stefan” Institute, Department of solid state physics, Ljubljana, Slovenia, <http://www.ijs.si/ijs/dept/epr/erssim.htm>) served for the evaluation and simulation of the EPR spectra. The amount of nitroxide released from the implant was determined by double integration of the recorded spectra and determination of the area under the curve of the obtained graphs.

### 2.2. In vitro studies

For *in vitro* monitoring of the *in situ* forming implant formation 200  $\mu$ l of the TB-containing polymer solution were injected through a 25 gauge needle into 50 ml of 0.1 M phosphate buffer (pH 7.4; 37 °C) placed in an incubation shaker (30 rpm). After injection into the buffer the implants formed immediately. At determined time points the implants were taken out the buffer and transferred to the EPR spectrometer. The EPR measurements were performed by an L-band spectrometer (MagnetTech, Germany) with a re-entrant resonator, operating at a microwave frequency of about 1.1–1.3 GHz. Measurements parameter were set to: modulation amplitude 0.14 mT, scan width 10 mT, scan time 30 s, centre field 49.1 mT, conversion time 0.2 ms, number of accumulations 3.

### 2.3. In vivo studies

All animal experiments followed a protocol approved by Animal Ethics Committee of the state Saxony–Anhalt, Germany. Female BALB/c mice (20–22 g) were housed under controlled conditions (12 h light/dark schedule, 24 °C) and received mice chow and tap water ad libitum. Prior to the EPR measurements the mice were fixed in special constructed polypropylene tubes, which facilitated repeated measurements without the use of anaesthesia. 100  $\mu$ l of the TB-containing polymer solution were injected subcutaneously through a 25 gauge needle in the femoral of the mice. Immediately after injection the mice were transferred to the EPR spectrometer and the first EPR spectra were recorded. After the measurement the mice were returned to the animal cage. At predetermined time intervals the femoral-implants were rescanned. The *in vivo* EPR measurements were performed by an L-band spectrometer (MagnetTech, Germany) equipped with a surface coil resonator, operating at a microwave frequency of about 1.1–1.3 GHz. Measurements parameter were set to: modulation amplitude 0.125 mT, scan width 10 mT, scan time 20 s, centre field 47.5 mT, conversion time 0.2 ms, number of accumulations 10.

## 3. Results and discussion

Typical parameters that could be obtained from EPR spectra are the hyperfine coupling parameter ( $2a_N$ ) and the rotational correlation

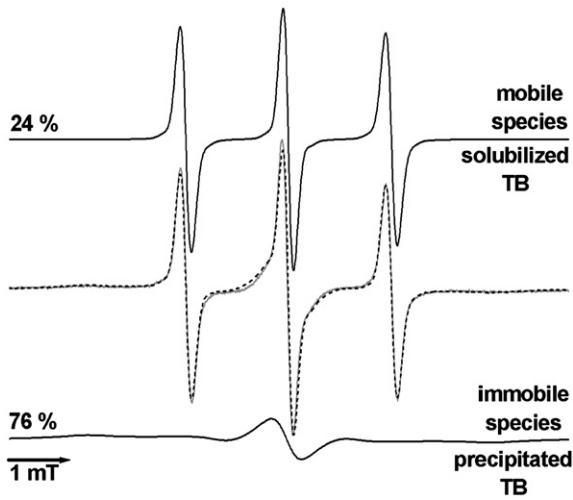


Fig. 2. EPR spectra of TB loaded implant exposed to phosphate buffer (grey) (after 30 min) and simulation (dashed line) of mobile (solubilized TB) and immobile (precipitated TB) spectral pattern.

time ( $t_c$ ). Magnetic interaction between the free electron and the nuclear spin ( $N=1$ ) of the nitrogen results in a hyperfine splitting of three lines (Fig. 2). The distance between the low and high field lines of the EPR spectrum ( $2a_N$ ) depends on the polarity of the nitroxide environment (Fig. 3 top). In regions with high polarity (e.g. water) the distance between the outer lines of the EPR spectra is increased, and

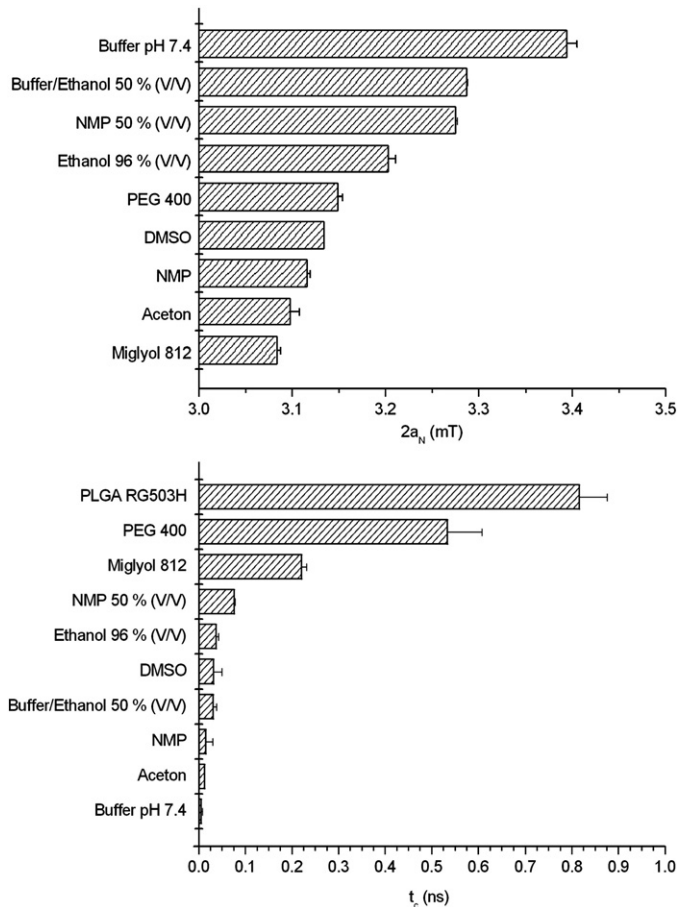


Fig. 3. Influence of environments with different polarities on the hyperfine splitting  $2a_N$  (top) and with different viscosities on the rotational correlation time  $t_c$  (bottom).

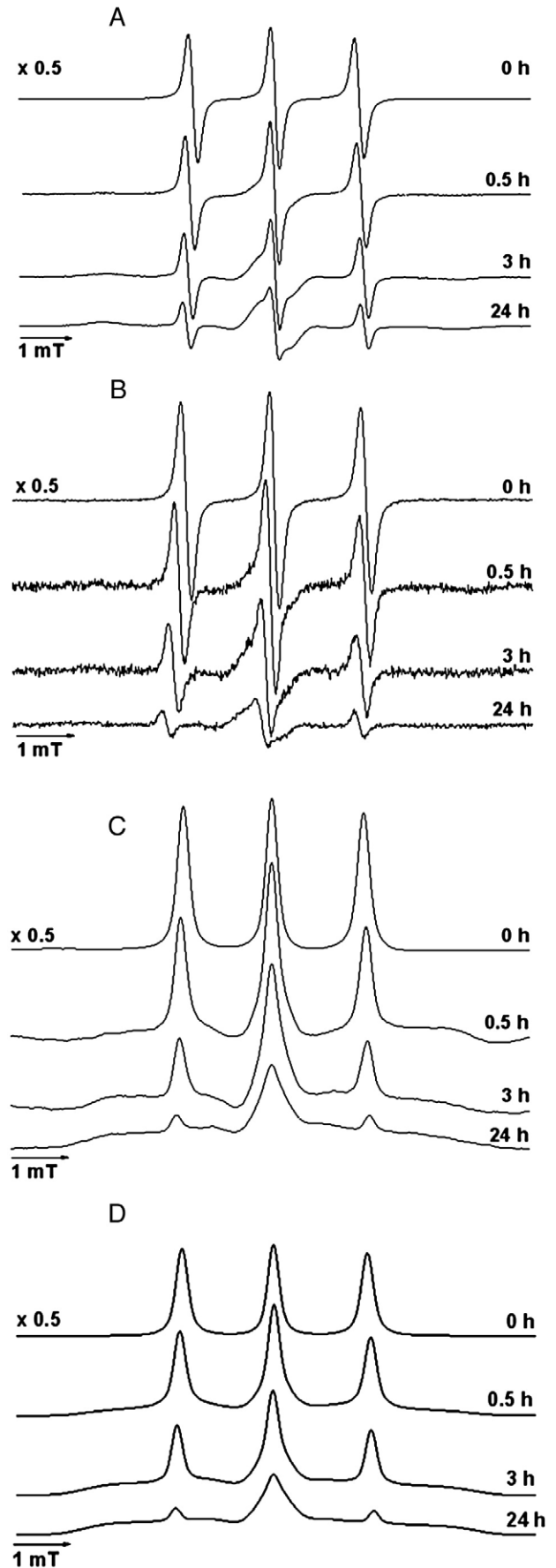


Fig. 4. EPR spectra of TB loaded implants exposed to phosphate buffer (A – recorded, C – integrated) or in mice (B – recorded, D – integrated).

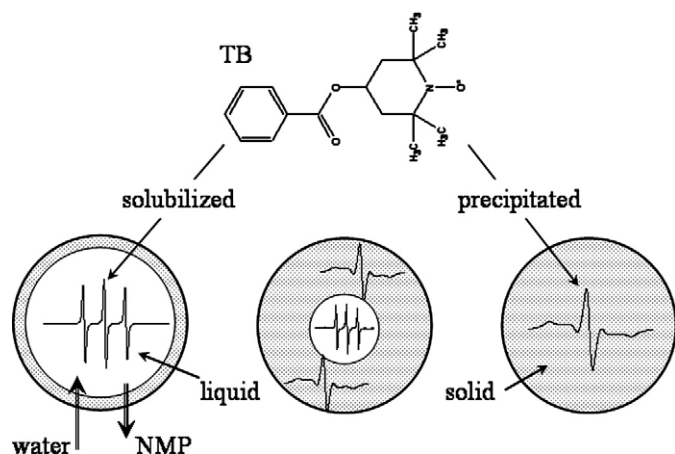


Fig. 5. Schematic illustration of the formation-mechanism of an injectable in situ forming system and chemical structure of tempolbenzoate (TB).

therefore the hyperfine coupling parameter, compared to region with low polarity (e.g. oil) [20]. The microviscosity, another parameter of the microenvironment, strongly influences the tumbling behaviour of the nitroxyl radicals. In low viscous media they tumble free, resulting in highly symmetric spectra with three narrow lines and rotational correlation times in the order of 0.01 to 0.1 ns (Fig. 3 bottom). Increasing the viscosity decreases the molecular tumbling rate of the nitroxide. Due to their restricted motion the anisotropy of the hyperfine interaction is only partially or not averaged, which results in a line broadening and a decrease of the signal amplitude (Fig. 2) and an increase in  $t_c$  (Fig. 3 bottom) [28,29].

The implant solutions were injected into buffer or mice and the changes in the EPR signals were monitored. The EPR spectra of the PLGA-NMP solutions indicated a highly mobile environment with the typical 3 sharp lines (Fig. 4) and rotational correlation times of  $0.095 \pm 0.015$  ns. The dissolved PLGA lead to a fourfold increase of the microviscosity of the NMP (rotational correlation time in pure NMP:  $0.022 \pm 0.003$  ns). After injection the NMP diffused into the surrounding aqueous environment, while water diffused into the PLGA matrix. PLGA precipitated and formed a solid implant with a NMP containing core inside (Fig. 5). The implant formation could be followed by EPR.

Fig. 2 shows EPR spectra from the PLGA-implant in vitro after 30 min of incubation with phosphate buffer. A superposition of two species within the spectra was detectable. TB precipitated within the PLGA and its mobility is restricted. The immobilization of TB results in so-called powder-like spectra (Fig. 2) with an increase in one order of

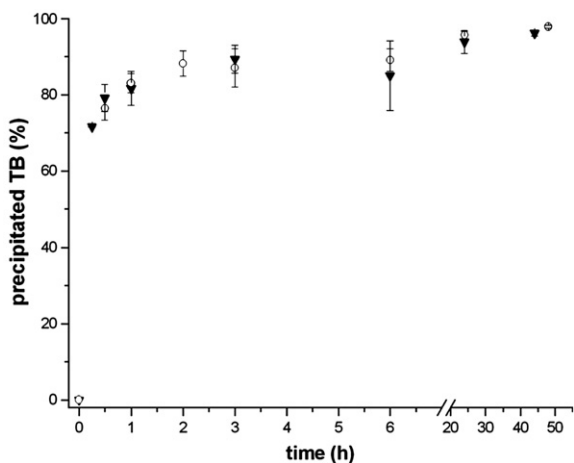


Fig. 6. *In vitro* (O) and *in vivo* (▼) distribution of precipitated TB in the implant during implant formation.

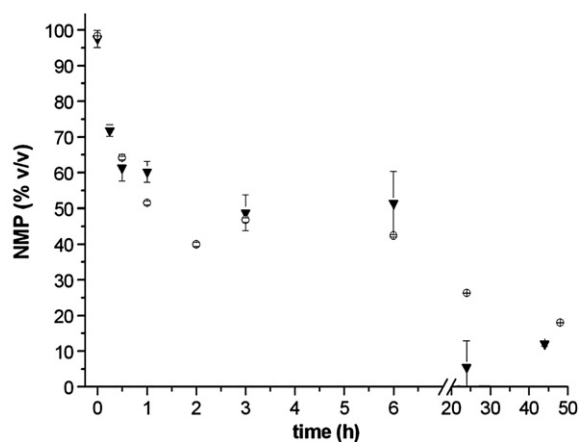


Fig. 7. *In vitro* (O) and *in vivo* (▼) kinetics of NMP-water exchange in the implant core (determined by EPR).

magnitude in  $t_c$  ( $0.816 \pm 0.060$  ns). About 24% of TB is still mobile and located in the NMP containing core at this time point, showing the same mobility as in the PLGA/NMP solution ( $0.096 \pm 0.033$  ns). Similar spectra were obtained from *in vivo* EPR measurements. The EPR spectrum, detected as the first derivative, is very sensitive to mobile nitroxides with their narrow lines. In superimposed spectra they are detectable below 1% [30]. Due to their broad lines and low signal amplitude, the immobilized TB is much more difficult to detect. It can

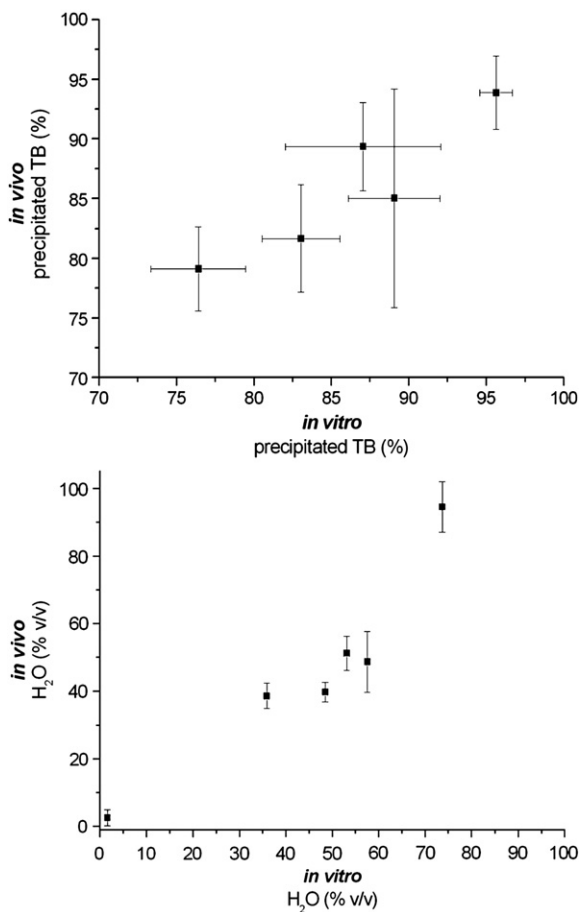


Fig. 8. *In vitro-in vivo* correlation of the kinetics of polymer precipitation (top) and NMP-water exchange (bottom).

be easily overlooked if only the first derivative (the most common form) of EPR spectra is considered. To increase the visibility of the immobilized (precipitated) species the EPR spectra were integrated. Fig. 4 shows TB spectra from the implants after different times of incubation in buffer or living mice in the recorded (first derivative) and integrated form. With increasing incubation time a decrease in the signal amplitude of the outer lines and line broadening was detectable *in vitro* and *in vivo*. The progress of implant solidification was quantified by simulation of the mobile and immobile species and determination of the proportion of the immobile spin probe (Fig. 6).

The precipitation of PLGA followed a two phase mechanism. Immediately after injection a thin PLGA shell was formed. NMP and TB dissolved in it diffused through the polymer shell into aqueous environment, while water diffused inside. At the same time the polymer matrix increased and TB precipitated. After 30 min  $24 \pm 3\%$  and  $28 \pm 3\%$  of the TB was immobilized within the polymer matrix, *in vitro* and *in vivo* respectively. Furthermore TB is located in an aqueous environment which is created via water penetration inside the implant. Due to the increasing hardening of the PLGA and further precipitation of the polymer the diffusion distances increased. According to the Einstein–Smoluchowski equation [31], where  $D$  is the diffusion coefficient,  $d$  the distance and  $t$  the time, with increasing diffusion distances inside the implant the time for diffusion of NMP outside and water inside the implant increased.

$$D = \frac{d^2}{2t} \rightarrow t = \frac{d^2}{2D}$$

Therefore proportion of immobilized TB increased much more slowly after 1 h ( $83.1 \pm 2.1$  *in vitro* and  $81.7 \pm 4.5$  *in vivo*), compared with after 6 h  $89.1 \pm 3.0$  *in vitro* and  $85.0 \pm 9.2$  *in vivo*. The implant formation is almost completed ( $95.6 \pm 1.0$  *in vitro* and  $94.0 \pm 3.0$  *in vivo*) after about 24 h. The remaining TB located in a mobile environment is supposed to be located in inner pores. The proportion of TB mobile in the matrix correlate with the total amount of released spin probe. We observe a strong burst effect followed by only moderate release. Within the first hour the TB content decreased to  $26.4 \pm 8.7\%$  and after 6 h still  $9.9 \pm 5.6\%$  of the spin probe were detectable *in vivo*. To assure that no spin probe containing buffer interferes with the determination of the TB distribution inside the implant, adsorbed buffer was carefully removed prior to the *in vitro* measurements. The EPR signals observed *in vivo* are only caused by TB incorporated in the implant, because released TB molecules diffuse rapidly into the surrounding tissue or blood stream where a rapid reduction to the EPR silent hydroxylamine occurs. Our results are supported by experiments from McHugh et al., who described the formation of a rigid, interconnecting porous structure framed by a polymer skeleton [13]. They observed an initial burst effect of human growth hormone followed by prolonged period of little protein release. The initial burst was correlated with the rapid diffusion of the protein in or near these interconnecting pores, while the slower long time release is due to protein entrapped in the hardening polymer. The replacement of NMP by water is another critical step during implant formation and strongly influences the drug release.

Alterations in the surrounding micropolarity of TB can be detected via the hyperfine splitting parameter  $2a_N$ . The higher the water content, the more polar the environment of TB, the larger is the distance between the 1st and the 3rd peak. Therefore the values  $2a_N$  were determined from the spectra and were plotted against the concentrations of NMP in different NMP–buffer mixtures (Fig. 1). The micropolarities of the implants were determined from the obtained calibration curve indicating the amount of NMP that was replaced by water. Within 1 h water penetrated into the implant and replaced approx. 50% of the NMP *in vitro* inside the PLGA–implant (Fig. 7). *In vivo* the velocity of the NMP–water exchange was slightly slower; where approximately 60% of the NMP was displaced by water. Further

exchange is slowed down corresponding with the observed reduced polymer precipitation velocity.

The kinetics of solvent exchange (Fig. 7) and polymer precipitation (Fig. 6) showed similar behaviour and good *in vitro*–*in vivo* correlation (Fig. 8). The initial faster *in vitro* water influx rate could be associated with a higher volume of the aqueous environment. Remarkably over 25% of the NMP is still incorporated into the implants after 24 h *in vitro*, compared to about 10% *in vivo*. This fact may be caused by the irregular shape of the implants, formed depending on the subcutaneous cavity into which they were injected. The shape determines the way of diffusion and therefore the exchange rates. Due to increasing polymer precipitation, this effect is more pronounced in later steps of implant formation. To quantify the remaining NMP is important for the development and characterization of ISFI for protein delivery. For example leuprolide acetate tends to aggregation when dissolved in NMP [16].

#### 4. Conclusions

Although solutions of poly(lactide-co-glycolide) (PLGA) in organic solvents have been extensively investigated as novel drug depots in the recent years, there exist, to the best of our knowledge, no systemic quantitative investigations about the mechanisms of implant formation *in vivo*. Therefore EPR was applied to shed more light into these in situ forming drug delivery systems. For the first time it was possible to detect implant formation online, non-invasively and continuously both *in vitro* and *in vivo* in living mice. The precipitation of a model drug substance within the polymer was monitored, following a two step mechanism. Furthermore the replacement of the organic solvent NMP by water was clearly demonstrated by polarity shifts within the implant and could be quantified. The ability to quantify the remaining organic solvent gives us a unique opportunity to assess the stability of sensitive drug molecules, like proteins, in these formulations. Both the kinetic of NMP–water exchange and polymer precipitation showed good *in vitro*–*in vivo* correlation. Further the EPR data suggest that drug release from in situ forming implants is a complex mechanism including water penetration and drug diffusion. These results help to understand mechanisms of implant formation and drug release. The presented non-destructive EPR method gives unique information about the micropolarity and microviscosity inside in situ delivery systems *in vivo* and can be used as a valuable tool of their development and optimization.

#### References

- [1] S. Tamilvanan, Oil-in-water lipid emulsions: implications for parenteral and ocular delivering systems, *Prog. Lipid Res.* 43 (2004) 489–533.
- [2] A. Sharma, U.S. Sharma, Liposomes in drug delivery: progress and limitations, *Int. J. Pharm.* 154 (1997) 123–140.
- [3] A.N. Lukyanov, V.P. Torchilin, Micelles from lipid derivatives of water-soluble polymers as delivery systems for poorly soluble drugs, *Adv. Drug Deliv. Rev.* 56 (2004) 1273–1289.
- [4] S. Thatte, K. Datar, R.M. Ottenbrite, Perspectives on: polymeric drugs and drug delivery systems, *J. Bioact. Compat. Polym.* 20 (2005) 585–601.
- [5] S. Freiberg, X.X. Zhu, Polymer microspheres for controlled drug release, *Int. J. Pharm.* 282 (2004) 1–18.
- [6] E. Ruel-Gariepy, J.C. Leroux, In situ-forming hydrogels – review of temperature-sensitive systems, *Eur. J. Pharm. Biopharm.* 58 (2004) 409–426.
- [7] A. Hatefi, B. Amsden, Biodegradable injectable in situ forming drug delivery systems, *J. Control. Release* 80 (2002) 9–28.
- [8] C.B. Packhaeuser, J. Schnieders, C.G. Oster, T. Kissel, In situ forming parenteral drug delivery systems: an overview, *Eur. J. Pharm. Biopharm.* 58 (2004) 445–455.
- [9] S. Einmahl, S. Capancioni, K. Schwach-Abdellaoui, M. Moeller, F. Behar-Cohen, R. Gurny, Therapeutic applications of viscous and injectable poly(ortho esters), *Adv. Drug Deliv. Rev.* 53 (2001) 45–73.
- [10] B. Balakrishnan, A. Jayakrishnan, Self-cross-linking biopolymers as injectable in situ forming biodegradable scaffolds, *Biomaterials* 26 (2005) 3941–3951.
- [11] D. Cohn, A. Sosnik, S. Garty, Smart hydrogels for in situ generated implants, *Biomacromolecules* 6 (2005) 1168–1175.
- [12] L.W. Wang, S. Venkatraman, L. Kleiner, Drug release from injectable depots: two different in vitro mechanisms, *J. Control. Release* 99 (2004) 207–216.
- [13] K.J. Brodbeck, S. Pushpala, A.J. McHugh, Sustained release of human growth hormone from PLGA solution depots, *Pharm. Res.* 16 (1999) 1825–1829.

- [14] O. Sator, M.K. Dineen, R. Perez-Marreno, F.M. Chu, G.J. Carron, R.C. Tyler, An eight-month clinical study of LA-2575 30,0 mg: a new 4-month, subcutaneous delivery system for leuprolide acetate in the treatment of prostate cancer, *Urology* 62 (2003) 319–323.
- [15] H.B. Ravivarapu, K.L. Moyer, R.L. Dunn, Parameters affecting the efficacy of a sustained release polymeric implant of leuprolide, *Int. J. Pharm.* 194 (2000) 181–191.
- [16] W.Y. Dong, M. Körber, V. Lopez Esguerra, R. Bodmeier, Stability of poly(D,L-lactide-co-glycolide) and leuprolide acetate in-situ forming drug delivery systems, *J. Control. Release* 115 (2006) 158–167.
- [17] X. Luan, R. Bodmeier, Influence of the poly(lactide-co-glycolide) type on the leuprolide release from in situ forming microparticle systems, *J. Control. Release* 110 (2006) 266–272.
- [18] P.D. Graham, K.J. Brodbeck, A.J. Mchugh, Phase inversion dynamics of PLGA solutions related to drug delivery, *J. Control. Release* 58 (1999) 233–245.
- [19] K.J. Brodbeck, J.R. DesNoyer, A.J. Mchugh, Phase inversion dynamics of PLGA solutions related to drug delivery — Part II. The role of solution thermodynamics and bath-side mass transfer, *J. Control. Release* 62 (1999) 333–344.
- [20] D.J. Lurie, K. Mäder, Monitoring drug delivery processes by EPR and related techniques - principles and applications, *Adv. Drug Del. Rev.* 57 (2005) 1171–1190.
- [21] K. Mäder, G. Bacic, A. Domb, O. Elmalak, R. Langer, H.M. Swartz, Noninvasive in vivo monitoring of drug release and polymer erosion from biodegradable polymers by EPR spectroscopy and NMR imaging, *J. Pharm. Sci.* 86 (1997) 126–134.
- [22] K. Mäder, B. Gallez, K.J. Liu, H.M. Swartz, Non-invasive in vivo characterization of release processes in biodegradable polymers by low-frequency electron paramagnetic resonance spectroscopy, *Biomaterials* 17 (1996) 457–461.
- [23] V.V. Khramtsov, Biological imaging and spectroscopy of pH, *Curr. Org. Chem.* 9 (2005) 909–923.
- [24] K. Mäder, S. Nitschke, R. Stösser, H.H. Borchert, A. Domb, Non-destructive and localized assessment of acidic microenvironments inside biodegradable poly-anhydrides by spectral spatial electron paramagnetic resonance imaging, *Polymer* 38 (1997) 4785–4794.
- [25] S. Siepe, W. Herrmann, H.H. Borchert, B. Lueckel, A. Kramer, A. Ries, R. Gurny, Microenvironmental pH and microviscosity inside pH-controlled matrix tablets: an EPR imaging study, *J. Control. Release* 112 (2006) 72–78.
- [26] S. Li, Hydrolytic Degradation Characteristics of Aliphatic polyesters derived from Lactic and Glycolic Acids, *J. Biomed. Mater. Res.* 48 (1999) 342–352.
- [27] A. Rube, S. Klein, K. Mäder, Monitoring of in vitro fat digestion by electron paramagnetic resonance spectroscopy, *Pharm. Res.* 23 (2006) 2024–2029.
- [28] A. Besheer, K.M. Wood, N.A. Peppas, K. Mäder, Loading and mobility of spin-labeled insulin in physiologically responsive complexation hydrogels intended for oral administration, *J. Control. Release* 111 (2006) 73–80.
- [29] K. Mäder, B. Bittner, Y.X. Li, W. Wohlauf, T. Kissel, Monitoring microviscosity and microacidity of the albumin microenvironment inside degrading microparticles from poly(lactide-co-glycolide) (PLG) or ABA-triblock polymers containing hydrophobic poly(lactide-co-glycolide) A blocks and hydrophilic poly(ethylene-oxide) B blocks, *Pharm. Res.* 15 (1998) 787–793.
- [30] K. Mäder, Characterization of nanoscaled drug delivery systems by electron spin resonance (ESR), *Nanosystem Characterization Tools in the Life Science*, Wiley-VCH, Weinheim, 2006, pp. 241–258.
- [31] P.W. Atkins, *Physical Chemistry*, VHC VerlagsgesellschaftmbH, Weinheim, 1990.